SCIENTIFIC REPORTS

OPEN

SUBJECT AREAS:
POLLUTION REMEDIATION
POPULATION SCREENING

Received
25 June 2014

Accepted
31 October 2014

Published
24 November 2014

Correspondence and requests for materials should be addressed to T.P. (pradeep@iitm.ac.in)

* These authors contributed equally to this work.

† Current Address: IMPRS MCB, Max-Planck Institute for Immunobiology and Epigenetics, 79108, Freiburg, Germany.

Antimicrobial silver: An unprecedented anion effect

J. R. Swathy[1]*, M. Udhaya Sankar[2]*, Amrita Chaudhary[2], Sahaja Aigal[1]†, Anshup[2] & T. Pradeep[1]

[1]DST Unit of Nanoscience (DST UNS) and Thematic Unit of Excellence (TUE), Department of Chemistry, Indian Institute of Technology Madras, Chennai 600036, India, [2]InnoNano Research, Chennai 600020, India.

Silver is an indispensable metal but its use has to be minimised for sustainable growth. Much of the silver lost during use is unrecoverable; an example being its use as an antimicrobial agent, a property known since ages. While developing methods to create an affordable drinking water purifier especially for the developing world, we discovered that 50 parts per billion (ppb) of Ag^+ released continuously from silver nanoparticles confined in nanoscale cages is enough to cause antimicrobial activity in conditions of normal water. Here we show that the antibacterial and antiviral activities of Ag^+ can be enhanced ~1,000 fold, selectively, in presence of carbonate ions whose concentration was maintained below the drinking water norms. The protective layers of the organisms were affected during the carbonate-assisted antimicrobial activity. It is estimated that ~1,300 tons of silver can be saved annually using this new way to enhance its antimicrobial activity.

Silver exhibits unique optical, catalytic, sensing and antimicrobial properties due to which its industrial demands, pegged at 16,000 to 24,000 tons per year[1], are estimated to grow at 12.5% annually[2]. Silver, as an antimicrobial agent is expected to have an annual demand of 3125 tons/year for medicine and 2800 tons/year in the fields of 'food, hygiene and water purification'[3]. Of the silver consumed in industrial processes, only 36% is recycled and the remaining is let out to the environment[4]. With increasing demands, production from the mines might not be sufficient. Silver is traditionally used as a disinfectant in delivering safe portable water to world[5] against severe gastroenteritis-causing pathogens, which are the second leading cause of death in children under the age of five. United Nations Children's Fund (UNICEF) claims that about 9% of global child deaths are due to diarrhoea. World Health Organization (WHO) estimates that gastroenteritis infection is responsible for 760,000 child deaths every year. Among the developing countries, India accounts for the highest number of diarrhoeal deaths (>24%), with 100,000 child deaths annually[6]. Biochemical properties of silver in the ionic form, against pathogens like bacteria, virus, fungi and protozoa have been widely studied and the reaction products silver may produce are less harmful compared to other disinfectants which produce disinfection by-products (DBPs). Complexity of contaminants, growth of population, emergence of resistive pathogens and their impact on the environment have led to the demand for advanced technologies for clean and safe drinking water[7]. Several trihalomethanes, haloacetic acids, haloacetonitriles, haloketones and other DBPs were found to cause colon, rectal and bladder cancers and adverse reproductive disorders, because of which the US EPA initiated a rule in the year 1992 to evaluate the need for additional controls for microbial pathogens and DBPs. The goal of this rule was to develop an approach that would reduce the level of exposure from disinfectants and DBPs, simultaneously controlling microbial pathogens[8]. Such technologies to reach the masses should not only be efficient but also affordable and thus silver ion-based commercial water purification units are evolving[9]. Therefore, it is appropriate to reduce the consumption of silver in view of the anticipated crisis in silver production and the current study points to a direction in this context.

In this work, we demonstrate the effectiveness of a synergetic combination of Ag^+ with the anion, CO_3^{2-} which enhances the antimicrobial activity. The concentration of silver used in water purification is differently stated by authors, but generally up to a maximum of 1 ppm[10]. For a specific silver ion concentration, the antimicrobial performance is in the order, seawater ≤ high organic matter-containing water ≤ high divalent cation-containing water ≤ synthetic water[11] due to the speciation of Ag^+. Active-silver, the concentration of effective ionic silver available for interaction with microbes in test water conditions varies with water quality. In this work, we initially focused on experiments to optimize the concentration of carbonate below the drinking water norms (secondary standard, United States Environmental Protection Agency, US EPA) while reducing the active-silver concentration, maintaining effective antimicrobial activity. The results were confirmed by further experiments and the mode of action was analysed. *Escherichia coli* and MS2 bacteriophage, the surrogates for water borne pathogens

(bacteria and viruses, respectively) were used for antimicrobial testing. The Ag^+ ion treatment was aimed for cent percent removal of coliforms and coliphages[12].

Results

Effect of speciation on the antimicrobial property of Ag^+. Initially, in the natural drinking water, spiked with an input bacterial load of 10^5 colony forming units (CFU)/mL (typical natural drinking water sources contain a maximum of 10^2–10^3 CFU/mL, in rural India), certain quantity of Ag^+ (in the range of 10 to 100 ppb) was added separately and the microbial survival was tested after a contact time of 1 h. A concentration of 50 ppb was found to be the active Ag^+ input concentration needed for maximum antibacterial activity (up to 99%), in natural drinking water. Even at an enhanced concentration of 1 ppm Ag^+, the residual microbial concentration was not diminished. It is important to note that chloride ions invariably present in natural water (1–250 ppm) leads to speciation of Ag^+ and thus reduces the availability of silver ions. Silver chloride complexes [AgCl (aq), $(AgCl)Ag^+$, $(AgCl)Cl^-$, $(AgCl)_n$ and their aggregates) due to their negative charge are nearly 300 times less in toxicity to bind with bacterial surface when compared to free silver ions[13]. With increasing concentrations of chloride ions (up to 200 ppm as in natural waters) at a fixed silver ion concentration, the speciation increases leading to a drop in the performance of bactericidal activity. At 200 ppm of Cl^-, silver exists as 0.16% of $[AgCl_3]^{2-}$, 31% of $[AgCl_2]^-$, 63% of AgCl (aq), and only 5.8% of input silver remains as Ag^+ (Supplementary Fig. S1). With Ag^+ alone, no significant antiviral activity was observed for MS2 bacteriophage in tap water. Silver in the ionic form continue to be available during the period of antimicrobial activity in the test water conditions (Supplementary Fig. S2).

Synergy of anions with silver's antimicrobial property. The residual microbial concentration (to the extent of 1% or 10^3 CFU/mL of *E. coli* and essentially all of the input viral load) still present is a challenge for reliable water purification. To address this economically and sustainably, the above method was improved upon. To 50 ppb Ag^+, various anions, namely NO_3^-, SO_4^{2-}, SiO_4^{2-}, PO_4^3, I^-, Br^- and CO_3^{2-} (or species derived from them, at prevalent conditions), as many of them can also be present in natural waters, were added at varying amounts to achieve a cent percent potential system. Among these, SiO_4^{2-} and CO_3^{2-} were promising compared to other anions, and the latter was more significant in this property. Therefore, the experiments were designed to reduce the Ag^+ concentration to a minimum at acceptable CO_3^{2-} levels, sufficient to kill bacterial and viral cells in the natural drinking water. It is important to note that antimicrobial activity due to carbonate alone was insignificant even at 100 mM (10,000 ppm) Na_2CO_3. However, we found that in presence of CO_3^{2-}, 50% lower concentration of silver i.e., 25 ppb Ag^+, was enough to obtain a complete (100,000 times) reduction in the input bacterial load (Supplementary Fig. S3). Therefore, while 50 ppb Ag^+ showed a 100 times reduction (from 10^5 CFU/mL to 10^3 CFU/mL), a combination of 25 ppb Ag^+ + 20 ppm CO_3^{2-} showed 100,000 times reduction (from 10^5 CFU/mL to 10^0 CFU/mL) resulting in 1,000 times enhanced antimicrobial effect.

In order to explain the carbonate's promotional activity, a combined Ag^+ (25 ± 10 ppb) and CO_3^{2-} (20 ± 5 ppm) release device was prepared, using silver nanoparticle (AgNP)-loaded biopolymer composite[14] and a sodium carbonate pellet, respectively. The output water from the device was spiked with *E. coli* and MS2 bacteriophage at required concentrations following which the water was tested for microbial survival (see Methods). In presence of CO_3^{2-} (~20 ppm) the combination was found to possess a significant antimicrobial activity at concentrations of Ag^+ as low as 20 ± 10 ppb within a contact time of 15 min. Thus CO_3^{2-} not only minimizes the concentration of silver required, but also increases the kinetics of the reaction (Supplementary Fig. S4). The combination was also tested for antibacterial activity against a gram positive organism, *Staphylococus aureus* at similar bacterial load used for *E. coli*. Pour plate experiments showed that the antibacterial property of the combination was similar for both gram positive and gram negative bacteria. In order to confirm the bactericidal activity of this combination, the water was given a standing time of 24 h and tested for bacterial viability. The overnight standing experiments showed that the combination acted as bactericidal agent and not as bacteriostatic (Supplementary Fig. S5). The combination was tested for cytotoxicity on human rhabdomyosarcoma RD cells and no such effect was seen.

Antiviral property of the combination. Considering the fact that the major water purification technique used for virus removal is the addition of chlorine which produces harmful DBPs, we propose that the $Ag^+ + CO_3^{2-}$ combination, in addition could also serve as an alternative to reduce pathogenic viruses by a safer method. Here, we tested the combination for antiviral property on MS2 phage. A sequential time interval study of 50 ppb Ag^+ alone and a combination of 50 ppb Ag^+ and 20 ppm CO_3^{2-} was performed (see Methods). We observed that while 50 ppb Ag^+ alone (even after 1–2 h contact) was unable to affect the phage, the combination of 50 ppb Ag^+ and 20 ppm CO_3^{2-} was found to achieve effective antiviral property within a contact time of 15 min (Supplementary Fig. S6). Moreover, by this study, we proved that this combination can handle virus at concentrations likely in ground water (10^3 plaque forming units (PFU)/mL) but can also efficiently control comparatively higher concentrations (~10^6 PFU/mL) that can prevail in non-portable water (Supplementary Fig. S7).

Compromised cell membrane/viral capsid. A defective outer membrane/capsid is suspected as the reason for enhanced activity of the combination. In order to confirm this, we conducted detailed dark field fluorescence imaging of bacteria and transmission electron microscopy of the viruses. Fluorescent staining experiments using dark field microscopy can distinguish between intact and membrane-permeable cells using LIVE/DEAD Baclight™ bacterial viability kit. The two stains used were the membrane impermeant, propidium iodide (PI), causing red fluorescence of membrane permeabilized cells and SYTO 9, a nucleic acid binding green fluorescent dye that could enter into all the cells regardless of whether they were intact or permeabilized. Defective PI fluorescing bacteria were observed as red when they were treated with $Ag^+ + CO_3^{2-}$ whereas untreated and Ag^+-treated bacteria (partly) show SYTO 9 emission (green) (Fig. 1 i, ii). Membrane permeabilization is seen in all the bacteria upon treatment with $Ag^+ + CO_3^{2-}$ (Fig. 1 C, F). We note that this happens for both *E. coli* and *S. aureus*, showing the effectiveness of the composition for gram negative and gram positive bacteria. Similarly, uranyl acetate stain enters defective viral capsids. Therefore, distinct difference in contrast is observed for carbonate-treated and untreated viruses under transmission electron microscopy (TEM)[15]. Dense dark centred capsids (defective capsids) which had taken up the uranyl acetate stain were seen in the $Ag^+ + CO_3^{2-}$ treated virus whereas untreated/Ag^+ treated viruses were found to be rigid which did not show the stain (Fig. 1 iii). These experiments prove that there is a significant damage to the outer protective layer of the bacterial/viral membrane as a result of $Ag^+ + CO_3^{2-}$ treatment.

Uptake of silver by bacteria/virus. Enhancement that carbonate creates on silver's antimicrobial performance was confirmed by studying the changes in Ag^+ uptake by bacteria and viruses, using inductively coupled plasma mass spectrometry (ICP MS). In these experiments, the bacteria and viruses, after treatment with Ag^+ and $Ag^+ + CO_3^{2-}$ at various incubation times were separated carefully and the filtrates were analyzed accurately for their silver content.

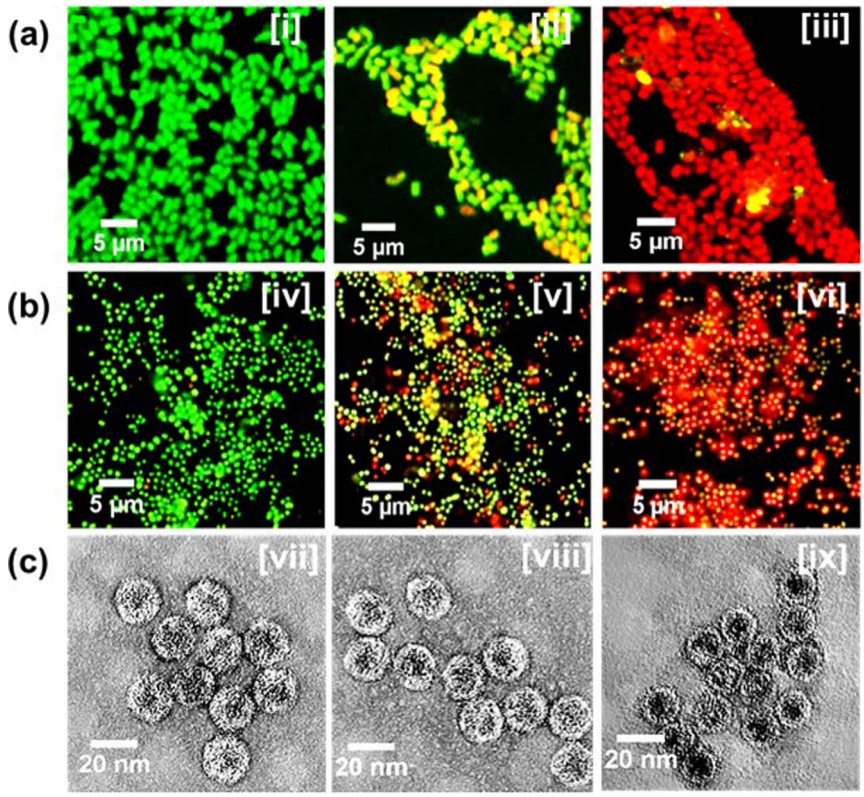

Figure 1 | The fluorescence microscopy and HRTEM images demonstrating the defective outer membrane/capsid in microbes caused due to $Ag^+ + CO_3^{2-}$ treatment. Line (a): Fluorescence microscopy images of *E. coli*: ([i] Input bacteria, [ii] 50 ppb Ag^+-treated bacteria and [iii] 50 ppb Ag^+ + 20 ppm CO_3^{2-}-treated bacteria after staining with syto9 and propidium iodide. Line (b): Similar fluorescence microscopy images of *S. aureus*: [iv] Input bacteria, [v] 50 ppb Ag^+-treated bacteria and [vi] 50 ppb Ag^+ +20 ppm CO_3^{2-}-treated bacteria. Line (c) TEM images of MS2 bacteriophage: [vii] Input viruses, [viii] 50 ppb Ag^+-treated viruses and [ix] 50 ppb Ag^+ + 20 ppm CO_3^{2-}-treated viruses after staining with 0.2% uranyl acetate. Images (vii) and (viii) appear the same as they are not damaged, while image (ix) appears dark as damage in the capsid allowed the stain to pass through it.

Appropriate blanks were conducted. The bacteria and viruses showed intake of Ag^+ up to 90% (±5%) in presence of CO_3^{2-} within a contact time of 10 min, whereas in its absence, the intake was less than 50% (Fig. 2). ICP MS results showed that the rate of uptake is an order of magnitude larger with carbonate ($k_{(Ag+)} = 0.0001$, $k_{(Ag+ +CO3)} = 0.001$ (both in min^{-1}), assuming a first order process.

Effect of pH change on Ag^+. Considering that the increase in the pH (from 7.0 to 8.5) due to the addition of CO_3^{2-} might be the reason behind this enhancement in the antibacterial effect of Ag^+, we performed experiments in natural drinking water with an adjusted pH of 8.5 using NaOH. The treated output was examined for microbial viability. Results of several experiments concluded that the NaOH-induced pH change did not enhance the antimicrobial activity of Ag^+.

Target of carbonate ions. The enhanced effect due to carbonate is suspected to be due to the peripheral proteins of the membrane. These peripheral proteins are associated with the membrane lipids and other proteins via electrostatic forces or hydrophobic interactions. Thus, conditions like high salt concentrations or an alkaline environment disrupt the interactions leading to the detachment of peripheral proteins[16]. The distinctive property of carbonate in the removal of peripheral membrane proteins of low molecular weight has been reported in animal cells[17] and *E. coli* K-12 cells[18]. Therefore, in presence of CO_3^{2-}, a disturbed membrane, free of peripheral proteins is suspected, which allows the penetration/cellular mobility of Ag^+, by increasing the bioavailability of silver ions. Fig. 3 is a schematic representation of this likely mechanism. In Fig. 3(i), bacteria are subjected to Ag^+ ions at a concentration ≤100 ppb. Ag^+ ions bind to negatively charged membrane proteins in a non-selective way and sufficient ions are unavailable to enter into cells to cause cell damage. In Fig. 3(ii), bacteria are subjected to Ag^+ at concentrations as low as 25 ppb along with 20 ppm CO_3^{2-}. In presence of CO_3^{2-}, several membrane-bound peripheral proteins are removed and thus Ag^+ binds directly to the cell surface. As a result, increased number of Ag^+ enter into the exposed cells and cause sufficient damage in them.

To verify this possibility, the treated bacteria were tested for the presence of low molecular weight membrane proteins/peptides using matrix-assisted laser desorption ionization time-of-flight mass spectrometry (MALDI TOF MS) (see Supplementary Note 1). Specific peaks at a set of m/z values (7,000–10,000) were observed in the control and Ag^+-treated bacterial cells whereas such peaks were completely absent in the case of carbonate-treated cells (Supplementary Fig. S8). The peaks obtained in the range of m/z 7,000–10,000 correspond to several proteins in *E. coli* which include both mature and immature proteins and peptides that are released from membrane bound proteins[19]. It is clear that carbonate, by acting upon membrane proteins/peptides, removes them. Removal of these membrane proteins increases the active-silver (as they offer a barrier for penetration by binding it) that leads to the total bioavailability of silver, in accordance with the uptake studies presented above. Separation of specific proteins responsible for the enhanced activity due to carbonate was difficult due to their reduced concentrations.

Discussion

In conclusion, the proposed combination of $Ag^+ + CO_3^{2-}$ yielded more than 100,000 times reduction in the case of bacteria and 1,000

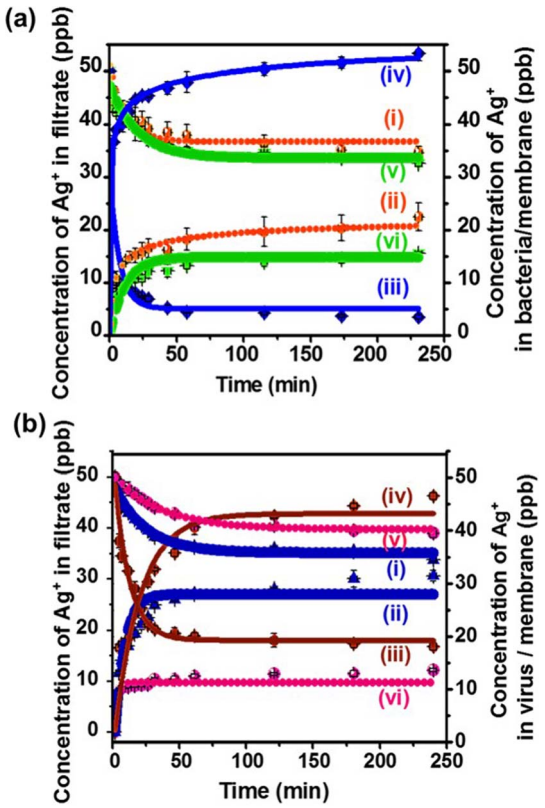

Figure 2 | ICP MS measurement of silver intake by bacteria and viruses. Concentration of silver in bacteria (a) and viruses (b) upon various treatments. Input concentration of silver is 50 ppb in the input water. Upon incubation with bacteria and viruses, Ag^+ concentration in the solution decreases while that in the organisms increase. These are plotted with time of incubation, measured by careful filtration through 100 kDa ultrafiltration membranes. After incubation with Ag^+; filtered water (i) and bacteria/viruses (ii). After incubation with $Ag^+ + CO_3^{2-}$; filtered water (iii) and bacteria/viruses (iv). Blank measurements without bacteria and viruses; filtered water (v); concentration on the membrane (vi). Measurements show that silver ion uptake is nearly quantitative; some loss of Ag^+ on the membrane as shown by trace (vi) is unavoidable as all membranes pick a small amount of silver. Sum of (i) and (ii) at 225 min does not give exactly 50 ppb due to this reason.

times reduction in the case of virus at concentrations as low as 25 ppb Ag^+ (Supplementary Fig. S9). In the absence of CO_3^{2-}, even double the concentration of silver (50 ppb) resulted in only 100 times reduction in the case of bacteria and negligible reduction in the case of virus. The mechanism behind the enhancement was found to be the disturbance caused to the cell by carbonate which targets the peripheral membrane proteins. Thus CO_3^{2-} exposed cells were disturbed and a lower concentration of Ag^+ was sufficient to cause complete cell damage. By reducing the Ag^+ concentration for antimicrobial activity, the unrecoverable release of metal ions into the environment is halved[20]. This work leads to a new paradigm in the field of affordable water purification by reducing the cost of antimicrobial treatment, particularly in the developing world, without disinfection by-products.

Methods

Testing protocol for antibacterial and antiviral efficacy. Natural drinking water condition was used for all the testing (Supplementary Table S1). Flasks containing 100 mL of water were spiked separately with 50 ppb Ag^+, 50 ppb Ag^+ + 20 ppm CO_3^{2-}, 20 ppm CO_3^{2-}, respectively and a bacterial load of $\sim 1 \times 10^5$ CFU/mL of *Escherichia coli* (ATCC 10536) was introduced into it. In the case of antiviral testing, $\sim 1 \times 10^3$ F-specific bacteriophage MS2 (ATCC 15597-B1) was used. Thereafter, the water was shaken gently and left for a contact time of 1 h and subsequently the viable microbial count was measured by conventional pour plate technique (for bacteria) and double layer plaque assay (for virus using *E. coli host C-3000* (ATCC 15597). Viable microbial counts were evaluated after an incubation period of 20–24 h at 37°C. In the case of gram positive organism, *Staphylococcus aureus* (ATCC 9144) was used at the same concentration. Corresponding control and blank experiments were maintained for each trial.

ICP MS Analysis. To flasks containing 100 mL of water, 50 ppb Ag^+, 50 ppb Ag^+ + 20 ppm CO_3^{2-} and 20 ppm CO_3^{2-} were spiked and bacteria/virus were added. 10 mL sample was collected at varying contact times and the cells were separated using polyvinylidene difluoride (PVDF) ultrafiltration membrane with molecular-weight cut-off of 100 kDa. The cells retained by the ultrafiltration membrane were suspended in 1 mL of millipore water and digested using HNO_3/H_2O_2. Concentration of Ag^+ present in both cells/viruses and the filtrate were measured using Perkin Elmer NexION 300X ICP MS. Careful standardization was performed.

Dark field Fluorescent Microscopic Analysis. Fluorescent microscopy imaging was performed using a Cytoviva microscopy system. For sample preparation, LIVE/DEAD Baclight™ bacterial viability kit (Molecular Probes, Eugene, OR)[13] was used. At each time point, 1 mL of the sample (50 ppb Ag^+, 50 ppb Ag^+ + 20 ppm CO_3^{2-} treated and control bacteria) was mixed with 2 μL of PI-SYTO 9 mix (1 : 1) and incubated in dark for 15 min. 0.5–1 μL sample was spotted on a 1 mm thick ultrasonically cleaned glass slide (SCHOTT) and it was covered with a 0.145 mm thick cleaned glass coverslip (SCHOTT). Imaging was performed using 100X oil (Cargille) immersion objective.

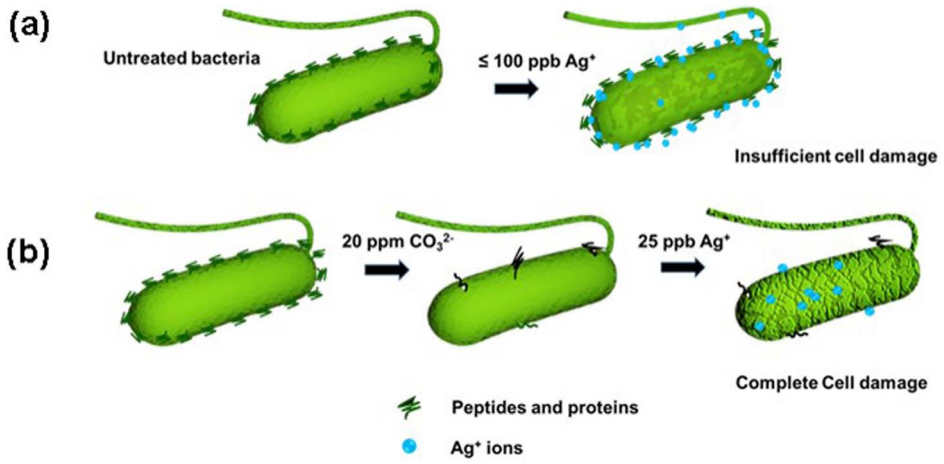

Figure 3 | Schematic representation of suspected mechanism behind the unprecedented enhancement of antimicrobial property of silver in presence of carbonate. (a) Healthy cells treated up to 100 ppb Ag^+ showed inadequate cell damage. (b) Healthy cells after exposed to 20 ppm CO_3^{2-} were damaged completely with 25 ppb Ag^+.

Transmission Electron Microscopy Analysis. Transmission electron microscopy (TEM) was carried out using a JEOL 3010 instrument with an ultra-high resolution (UHR) polepiece. TEM specimens were prepared by dropping one or two drops of the sample onto a paraffin tape and the carbon-coated copper grid was placed over it for 5 sec. After removing the excess sample, the grid was placed on a drop of 2% solution uranyl acetate in water for 5 sec and excess stain was blotted away. The grid was dried under ambient conditions[15]. Measurements were carried out at 100 kV.

1. Johnson, J. *et al.* Contemporary anthropogenic silver cycle: a multilevel analysis. *Environ. Sci. Technol.* **39**, 4655–4665 (2005).
2. GFMS Thomson Reuters. The outlook for silver's industrial demand. https://www.silverinstitute.org/site/wpcontent/uploads/2012/11/OutlookSilverDemand.pdf (2012). Date of access: 25/06/2014.
3. Gordon, R. B., Bertram, M. & Graedel, T. E. Metal stocks and sustainability. *Proc. Natl. Acad. Sci. U.S.A.* **103**, 1209–1214 (2006).
4. Rauch, J. N. & Pacyna, J. M. Earth's global Ag, Al, Cr, Cu, Fe, Ni, Pb, and Zn cycles. *Global Biogeochemical Cycles* **23**, 1–16 (2009).
5. Pradeep, T. & Anshup, S. Noble metal nanoparticles for water purification: A critical review. *Thin Solid Films* **517**, 6441–6478 (2009).
6. WHO media centre, Diarrhoeal disease. http://www.who.int/mediacentre/factsheets/fs330/en (2013). Date of access: 25/06/2014.
7. Schwarzenbach, R. P. *et al.* The challenge of micropollutants in aquatic systems. *Science* **313**, 1072–1077 (2006).
8. Sedlak, D. L. & von Gunten, U. The chlorine dilemma. *Science* **331**, 42–43 (2011).
9. Jayaraman, K. Pesticide filter debuts in India. *Chemistry World* **4**, 15–16 (2007).
10. Kumar, R. & Munstedt, H. Silver ion release from antimicrobial polyamide/silver composites. *Biomaterials* **26**, 2081–2088 (2005).
11. Zhang, H., Smith, J. A. & Craver, V. O. The effect of natural water conditions on the anti-bacterial performance and stability of silver nanoparticles capped with different polymers. *Water Res.* **46**, 691–699 (2012).
12. U.S. Environmental Protection Agency. National primary drinking water regulations. **EPA 816-F-09-004** www.epa.gov/safewater/consumer/pdf/mcl.pdf (2009). Date of access: 25/06/2014.
13. Choi, O. *et al.* The inhibitory effects of silver nanoparticles, silver ions and silver chloride colloids on microbial growth. *Water Res.* **42**, 3066–3074 (2008).
14. Sankar, M. U. *et al.* Biopolymer-reinforced synthetic granular nanocomposites for affordable point-of-use water purification. *Proc. Natl. Acad. Sci. U.S.A.* **110**, 8459–8464 (2013).
15. Brenner, S. & Horne, R. W. A negative staining method for the high resolution electron microscopy of viruses. *Biochem. Biophys. Acta* **34**, 103–110 (1959).
16. Hausman, R. E. C. & Cooper, G. M. *The Cell: A Molecular Approach*, (ed.) **2**, (ASM Press, Washington, D.C., 2000).
17. Fujiki, Y., Hubbard, A. L., Fowler, S. & Lazarow, P. B. Isolation of intracellular membranes by means of sodium carbonate treatment: Application to endoplasmic reticulum. *J. Cell Biol.* **93**, 97–102 (1982).
18. Molloy, M. P. *et al.* Proteomic analysis of the *Escherichia coli* outer membrane. *Eur. J. Biochem.* **267**, 2871–2881 (2000).
19. Meetani, M. A. & Voorhees, K. J. MALDI mass spectrometry analysis of high molecular weight proteins from whole bacterial cells: Pretreatment of samples with surfactants. *J. Am. Soc. Mass. Spectrom.* **16**, 1422–1426 (2005).
20. Eckelman, M. J. & Graedel, T. E. Silver emissions and their environmental impacts: A multilevel assessment. *Environ. Sci. Technol.* **41**, 6283–6289 (2007).

Acknowledgments

We thank Jyotisarita Mohanti and Anirban Som for their technical support in transmission electron microscopy. We thank R. Swathi and Ananya Baksi for their technical support in ICP-MS analysis and MALDI TOF measurements, respectively. We thank the Department of Science and Technology (Government of India) for constantly supporting our research program on nanomaterials.

Author contributions

T.P., J.R.S., A.C., M.U.S., S.A. and A designed the experiments, J.R.S., A.C., M.U.S., S.A. and A performed the experiments, T.P., J.R.S., A.C., M.U.S., S.A. and A analysed the data, wrote the paper.

Additional information

Supplementary information accompanies this paper at http://www.nature.com/scientificreports

Competing financial interests: The authors declare no competing financial interests.

How to cite this article: Swathy, J.R. *et al.* Antimicrobial silver: An unprecedented anion effect. *Sci. Rep.* **4**, 7161; DOI:10.1038/srep07161 (2014).